UNIVERSITY OF CALIFORNIA
RIVERSIDE

Disruption of Nuclear Receptor Signaling Alters Triphenyl Phosphate-Induced Cardiotoxicity in Zebrafish Embryos

A Thesis submitted in partial satisfaction
of the requirements for the degree of

Master of Science

in

Environmental Toxicology

by

Constance Ann Mitchell

December 2018

Thesis Committee:
Dr. David C. Volz, Chairperson
Dr. Daniel Schlenk
Dr. Prudence Talbot

The Thesis of Constance Ann Mitchell is approved:

_____

_____

_____

Committee Chairperson

University of California, Riverside

Dedication

This work is dedicated to my parents and to my husband, Arturo, whose love and support made my journey possible.

Acknowledgement

I would first and foremost like to express my gratitude to Dr. David C. Volz, whose mentorship, support, and guidance made this degree possible. I am indebted to him for giving me this opportunity to grow my knowledge base, research skills, and develop as a scientist professionally. He has opened many doors for me, and I have gained an invaluable supporter for all my future endeavors.

Additionally, I would like to thank my committee members, Drs. Daniel Schlenk and Prue Talbot for their insight and support throughout my degree.

I would also like to thank my lab members, past and present, especially Sara Frie Vliet, Dr. Subham Dasgupta, Aalekhya Reddam, Vanessa Cheng, and Dr. Allison Kupsco for their friendship and support. They have been instrumental in helping me through graduate school. I want to express my appreciation for Victoria McGruer, Dr. Luisa Becker Bertotto, Marissa Giroux and other Schlenk Lab members for their help.

Finally, I want to express my gratitude to my friends and family for their love and support. My parents, Bryon and Darlene, have given me unwavering support throughout all my schooling and in everything I do. My husband, Arturo, has always been there to motivate me and help me to succeed.

ABSTRACT OF THE THESIS

Disruption of Nuclear Receptor Signaling Alters Triphenyl Phosphate-Induced Cardiotoxicity in Zebrafish Embryos

by

Constance Ann Mitchell

Master of Science, Environmental Toxicology
University of California, Riverside, December 2018
Dr. David C. Volz, Chairperson

Triphenyl phosphate (TPHP) is an unsubstituted aryl phosphate ester used as a flame retardant and plasticizer within the United States. Using zebrafish as a model, the objectives of this study were to rely on (1) mRNA-sequencing to uncover pathways disrupted following embryonic TPHP exposure and (2) high-content screening to identify nuclear receptor ligands that enhance or mitigate TPHP-induced cardiotoxicity. Based on mRNA-sequencing, TPHP exposure from 24 to 72-h postfertilization (hpf) resulted in a concentration-dependent increase in the number of transcripts significantly affected at 72 hpf, and pathway analysis revealed that 5 out of 9 nuclear receptor pathways were associated with the retinoid X receptor (RXR). Based on a screen of 74 unique nuclear receptor ligands as well as follow-up experiments, 2 compounds—ciglitazone (a peroxisome proliferator-activated receptor gamma, or PPARγ, agonist) and fenretinide (a pan-retinoic acid receptor, or RAR, agonist)—reliably mitigated TPHP-induced cardiotoxicity in the absence of effects on TPHP uptake or metabolism. As these data suggested that TPHP may be activating RXR (a heterodimer for both RARs and PPARγ), we co-exposed embryos to HX 531—a pan-RXR antagonist—from 24 to 72 hpf and,

contrary to our hypothesis, found that co-exposure to HX 531 significantly enhanced TPHP-induced cardiotoxicity. Using a luciferase reporter assay, we also found that TPHP did not activate nor inhibit chimeric human RXRα, RXRβ, or RXRγ, suggesting that TPHP does not directly bind nor interact with RXRs. Overall, our data suggest that TPHP may interfere with RXR-dependent pathways involved in cardiac development.

Table of Contents

Title Page……i

Copy Right Page……ii

Signature Approval Page……iii

Dedication……iv

Acknowledgment……v

Abstract……vi

Table of Contents……viii

Figure Legend…….……ix

Introduction……1

Materials and Methods……4

Results……16

Discussion……34

References……40

FIGURE LEGEND

Figure 1: mRNA Sequencing Reveals That TPHP Disrupts RXR-Dependent Pathways ……..……..18

Figure 2: Fifteen Out of Seventy-Four Nuclear Receptor Ligands Mitigate TPHP-Induced Cardiotoxicity Following Co-Exposure From 24 to 72 hpf ……..……...…..22

Figure 3: Pretreatment With Ciglitazone or Fenretinide Mitigates TPHP-Induced Cardiotoxicity Activity ...……..…….....23

Figure 4: Co-exposure With Ciglitazone or Fenretinide Does Not Affect Embryonic Doses of TPHP or DPHP ……..…...26

Figure 5: Co-Exposure to a pan-RXR Antagonist (HX 531) From 24 to 72 hpf Enhances TPHP-Induced Cardiotoxicity ……..……..……...29

Figure 6: TPHP Is Not an Agonist Nor Antagonist of Human RXRα-, RXRβ-, or RXRγ Within CHO Cells……..…….…....32

INTRODUCTION

Nuclear receptors play an essential role in development within all vertebrates, acting as transcription factors at highly specific and coordinated stages within developing embryos (Chandler *et al*., 1983; McKnight and Palmiter, 1979; Polak and Domany, 2006; Rhinn and Dollé, 2012). In the vertebrate embryo, one of the first organs to form is the heart (Moorman *et al*., 2003), a process that is controlled by transcription factors, including homeobox (Schott *et al*., 1998), t-box (Basson *et al*., 1997), and nuclear receptor proteins (Mendelsohn *et al*., 1994). Retinoic acid receptors (RARs) are nuclear receptors necessary for many processes in cardiac development such as cell specification (Wobus *et al*., 1997), heart field patterning (Smith *et al*., 1997), and myocardial growth (Merki *et al*., 2005). RARs can be activated by many structurally different ligands (Blumberg *et al*., 1996), but most selectively by all-*trans* retinoic acid (Giguere *et al*., 1987). Upon activation, RARs heterodimerize with retinoid X receptors (RXRs), resulting in binding to retinoic acid response elements and transcription of genes necessary for cardiac development (Minucci *et al*., 1997). Optimal activation of RARs is necessary for proper cardiac development and morphogenesis, as excess or insufficient amounts of signaling both lead to cardiotoxicity (Chen *et al*., 2008; Li *et al*., 2016). Therefore, xenobiotics affecting the RAR signaling pathway—either directly or indirectly—can lead to cardiac malformations in developing embryos (Isales *et al.,* 2015; Paganelli *et al*., 2010).

Triphenyl phosphate (TPHP) is an unsubstituted aryl phosphate ester flame retardant and plasticizer with an estimated annual production between 10 and 50 million pounds in the United States (Brooke *et al*., 2009). TPHP is used in commercial products such as electronic wiring, plasticized vinyl polymers, automotive interiors, and furniture upholstery (van der Veen and de Boer, 2012). Similar to other additive flame retardants, TPHP can migrate out of end-use products and into indoor dust (Stapleton *et al*., 2009). TPHP is also used in nail polish and enamels, and one study demonstrated that, following application of TPHP-containing nail polishes, concentrations of the urinary metabolite of TPHP (diphenyl phosphate, or DPHP) were significantly increased in women (Mendelsohn *et al.*, 2016). Therefore, humans may be exposed to TPHP via inhalation, ingestion, and/or dermal exposure, although little is known about the potential effects of chronic exposure to human populations, particularly with respect to prenatal development.

Our previous findings demonstrated that TPHP blocks cardiac looping in zebrafish embryos (McGee *et al*., 2013). Interestingly, TPHP-induced cardiotoxicity is aryl hydrocarbon receptor-independent (McGee *et al*., 2013), and exposure of developing zebrafish to TPHP in the presence of nontoxic concentrations of a pan-RAR antagonist (BMS493) results in enhancement of cardiotoxicity, an effect that is not due to differential uptake or metabolism of TPHP (Isales *et al*., 2015). In addition, TPHP is a potent agonist for human peroxisome proliferator-activated receptor gamma (PPARγ) within cell lines

(Belcher *et al*., 2014; Pillai *et al*., 2014), and induces a significant increase in human PPARγ activity at nominal concentrations of >10 μM within cell culture media. As PPARγ and RARs are ligand-activated transcription factors that share RXR as a heterodimer (DiRenzo *et al*., 1997), activation of PPARγ may lead to increased recruitment of available RXR, decreased RAR/RXR heterodimerization, and repressed RAR function. However, little is currently known about how TPHP interferes with pathways regulated by PPARγ, RARs, RXRs, and other nuclear receptors, specifically during cardiac development. Using zebrafish as a model, the overall objective of this study was to identify other potential nuclear receptors involved in mediating TPHP-induced cardiotoxicity during embryonic development. To accomplish this objective, we relied on a combination of mRNA-sequencing, high-content screening, and human reporter assays to test the hypothesis that TPHP interferes with PPARγ- and RAR-mediated signaling pathways involved in cardiac development during zebrafish embryogenesis. In addition, we quantified embryonic doses of TPHP and DPHP—a primary TPHP metabolite—to confirm that TPHP uptake and metabolism was not affected by coexposure to two nuclear receptor ligands identified from this study.

MATERIALS AND METHODS

Animals

Adult wildtype (strain 5D) zebrafish were maintained on a recirculating system with UV sterilization and mechanical/biological filtration units (Aquaneering, San Diego, California), and were kept under a 14:10-h light-dark cycle at a water temperature of approximately 27°C–28°C, pH of approximately 7.2, and conductivity of approximately 900–950 µS. Water quality was constantly monitored for pH, temperature, and conductivity using a real-time water quality monitoring and control system. Ammonia, nitrate, nitrite, alkalinity, and hardness levels were manually monitored weekly by test strip (Lifeguard Aquatics, Cerritos, California). Zebrafish were fed once per day with dry diet (Gemma Micro 300, Skretting, Fontaine-lès-Vervins, France). Adult males and females were bred directly on-system using in-tank breeding traps suspended within 3-l tanks. For all experiments described, newly fertilized eggs were collected within 30 min of spawning, rinsed, and reared in a temperature-controlled incubator (28°C) under a 14:10-h light-dark cycle. All embryos were sorted and staged according to previously described methods (Kimmel *et al*., 1995). All adult breeders were handled and treated in accordance with an Institutional Animal Care and Use Committee-approved animal use protocol (No. 20150035) at the University of California, Riverside.

Chemicals

TPHP (99.5% purity) was purchased from ChemService, Inc. (West Chester, Pennsylvania), whereas fenretinide (>99.3% purity), ciglitazone (>99.4% purity), and HX 531 (>99.8% purity) were purchased from Tocris Bioscience (Bristol, UK). All stock solutions were prepared by dissolving chemicals in high performance liquid chromatography-grade dimethyl sulfoxide (DMSO), and stored at room temperature within 2-ml amber glass vials with polytetrafluoroethylene-lined caps. Embryo media (5 mM NaCl, 0.17 mM KCl, 0.33 mM $CaCl_2$, 0.33 mM $MgSO_4$) was prepared at pH 7. The SCREEN-WELL Nuclear Receptor Ligand Library was obtained from Enzo Life Sciences, Inc. (Farmingdale, New York). Stock solutions (100 µl of 1 or 10 mM stock per compound) of the Nuclear Receptor Ligand Library (1 deep-well, 96-well plate containing 74 compounds) were prepared and provided in DMSO by Enzo Life Sciences and stored at −30°C upon arrival. Tricaine methanesulfonate (MS-222) (Western Chemical, Inc., Ferndale, Washington) solutions were freshly made by dissolving MS-222 into embryo media. All working solutions were freshly prepared by spiking stock solutions into embryo media, resulting in 0.2% DMSO within all vehicle control and treatment groups.

High-content screening assays

Black 384-well microplates with 0.17-mm glass-bottom wells (Matrical Bioscience, Spokane, Washington) were used for all assays. Newly fertilized eggs were collected immediately following spawning and incubated in groups of

approximately 100 per plastic petri dish within a light- and temperature-controlled incubator until 24 h postfertilization (hpf). Viable embryos were transferred to a 384-well plate at 24 hpf, resulting in 1 embryo per well and 16 or 32 embryos per treatment depending on the experiment. Each well contained 50 µl of either vehicle (0.2% DMSO) or treatment solution. The plate was then covered with a plate lid, wrapped with parafilm to minimize evaporation, and incubated under static conditions at 28°C under a 14:10-h light-dark cycle until 72 hpf.

At 72 hpf, embryos were removed from the incubator and anesthetized with 100 mg/l MS-222 by adding 25 µl of 300 mg/l MS-222 to 50 µl of vehicle or treatment solution at 72 hpf. To help orient hatched embryos in right or left lateral recumbency, the plate was centrifuged at 200 rpm for 3 min. Using automated image acquisition protocols and parameters previously optimized (Yozzo *et al*., 2013) for our ImageXpress Micro XLS Widefield High-Content Screening System (Molecular Devices, Sunnyvale, California), each embryo was imaged to analyze the following endpoints: percent survival, percent hatch, pericardial area, and body length. Following completion of image acquisition, 72-hpf embryos were then euthanized by placing the plate at 4°C for 30 min.

Using MetaXpress 6.0.3.1658 software (Molecular Devices), body length (µm) and pericardial area (μm^2) were quantified using previously described protocols (Yozzo *et al*., 2013). Each well was inspected after imaging to assess embryo orientation and survival. Percent survival and hatch for each treatment group were recorded. Embryos that did not survive or hatch, as well as embryos that

were grossly malformed, were not included in the analysis for body length and pericardial area. Using these criteria only hatched and live embryos positioned in right or left lateral recumbency were analyzed.

Prior to conducting the nuclear receptor ligand library screen, we first conducted a range-finding exposure to identify a TPHP concentration that reliably blocked cardiac looping in the absence of effects on hatch rate and survival. A 50 mM stock of TPHP was prepared in 100% DMSO and then serially diluted by 1.25× to create 5.4, 6.7, 8.4, 10.5, 13.1, 16.4, 20.5, 25.6, 32, and 40 mM solutions. These solutions were spiked into embryo media, resulting in 1000-fold dilutions for each treatment group. Each treatment group consisted of 32 embryos exposed to either 0.2% DMSO or TPHP (5.4, 6.7, 8.4, 10.5, 13.1, 16.4, 20.5, 25.6, 32, 40, or 50 µM) from 24 to 72 hpf. At 72 hpf, embryos were anesthetized and imaged as described earlier. Based on this range-finding exposure, 20 µM TPHP was selected as a concentration that reliably blocked cardiac looping in the absence of effects on hatch rate and survival.

mRNA sequencing

To assess the potential effects of TPHP on the embryonic transcriptome at 72 hpf, 24-hpf embryos (30 embryos per petri dish; 6 petri dishes per treatment) were arrayed in clear petri dishes containing 10 ml of vehicle (0.2% DMSO) or TPHP (5, 10, or 20 µM). Embryos were incubated from 24 to 72 hpf at 28°C under a 14:10-h light-dark cycle and static conditions, snap-frozen in liquid nitrogen at 72 hpf, and stored at −80°C until RNA extraction. After combining 2

replicate petri dishes per pool, 3 replicate pools of up to 60 72-hpf hatched embryos per pool were homogenized in 2-ml cryovials using a PowerGen Homogenizer (Thermo Fisher Scientific, Waltham, Massachusetts), resulting in a total of 12 samples. Following homogenization, a SV Total RNA Isolation System (Promega, Madison, Wisconsin) was used to extract total RNA from each replicate sample per manufacturer's instructions.

Libraries were prepared using a QuantSeq 3' mRNA-Seq Library Prep Kit FWD (Lexogen, Vienna, Austria) and indexed by treatment replicate per manufacturer's instructions. Library quality and quantity were confirmed using a Qubit 2.0 Fluorometer and 2100 Bioanalyzer system, respectively. Libraries were then pooled, diluted to a concentration of 1.3 pM (with 1% PhiX control), and single-read (1X75) sequenced on our Illumina MiniSeq Sequencing System (San Diego, California) using a 75-cycle High-Output Reagent Kit. All sequencing data were uploaded to Illumina's BaseSpace in real-time for downstream analysis of quality control. Raw Illumina (fastq.gz) sequencing files (12 files totaling 1.14 GB) are available via NCBI's BioProject database under BioProject ID PRJNA416833, and a summary of sequencing run metrics are provided in Supplementary Table 1 (>90.3% of reads were ≥Q30). All 12 raw and indexed Illumina (fastq.gz) sequencing files were downloaded from BaseSpace, and uploaded to Bluebee's genomics analysis platform (https://www.bluebee.com) to align reads against the current zebrafish genome assembly (GRCz10). After combining treatment replicate files, a DESeq2 application within Bluebee (Lexogen Quantseq DE 1.2)

was used to identify significant treatment-related effects on transcript abundance (relative to vehicle controls) based on a false discovery rate (FDR) *p*-adjusted value < .01.

Using DESeq2-identified transcripts with a FDR *p*-adjusted value < .01, downstream analyses were run using Qiagen's Ingenuity Pathway Analysis (IPA) (Germantown, Maryland). Statistically significant transcripts were uploaded to IPA, and human, rat, and mouse homologs were automatically identified within IPA using NCBI's HomoloGene. A Tox Analysis was then performed using a Fisher's Exact Test *p*-value threshold of .05 as the basis for identifying statistically significant pathways; the algorithm considered both direct and indirect relationships using Ingenuity Knowledge Base (genes only) as the reference set.

Nuclear receptor ligand library screens

All 74 nuclear receptor ligands were first screened in the absence of TPHP for potential effects on survival, hatch, body length, and pericardial area at the limit concentration provided by Enzo within the SCREEN-WELL Nuclear Receptor Ligand Library. Ligand stocks (1 mM for 5 ligands; 10 mM for 69 ligands) were diluted in embryo media, resulting in final treatment concentrations of 1 or 10 µM. For each ligand, 16 embryos were exposed under static conditions from 24 to 72 hpf at 28°C under a 14:10-h light-dark cycle, and then anesthetized and imaged as described earlier. Ligands resulting in <75% survival or hatch, or statistically significant effects on body length and/or pericardial area, were rescreened at

1.25-fold dilutions to identify maximum tolerated concentrations (MTCs) based on survival, hatch, body length, or pericardial area.

After identifying the MTC for each ligand, embryos were treated with the MTC of each ligand in the presence or absence of 20 µM TPHP. Each 384-well plate contained a total of 24 treatment groups (1 embryo per well; 1 column per treatment; 16 embryos per treatment): vehicle (0.2% DMSO), 20 µM TPHP, 11 ligands at the MTC, and 11 ligands at the MTC + 20 µM TPHP. All embryos were treated under static conditions from 24 to 72 hpf at 28°C under a 14:10-h light-dark cycle, and then anesthetized and imaged as described earlier. Coexposures resulting in a statistically significant increase or decrease in pericardial area relative to 20 µM TPHP alone were repeated at least 3 times to confirm that results were reproducible.

If reproducible effects at MTCs were observed at least 2 out of 3 times, ligands were screened in concentration-response format using 3 concentrations per ligand (0.25×, 0.5×, or 1× MTC). Each 384-well plate contained a total of 8 treatment groups (one embryo per well; 1 column per treatment; 16 embryos per treatment): vehicle (0.2% DMSO), 20 µM TPHP, or 3 concentrations per ligand (0.25×, 0.5×, or 1× MTC) in the presence or absence of 20 µM TPHP. All embryos were treated under static conditions from 24 to 72 hpf at 28°C under a 14:10-h light-dark cycle, and then anesthetized and imaged as described earlier. Co-exposures resulting in a concentration-dependent increase or decrease in

pericardial area relative to 20 µM TPHP alone were repeated at least twice to confirm that results were reproducible.

Ciglitazone and fenretinide pretreatments

Using clear 96-well assay plates (Corning Incorporated, Corning, New York) containing 2 embryos per well, embryos were pretreated with 300 µl of vehicle (0.2% DMSO), 5.24 µM ciglitazone, or 2.14 µM fenretinide from 24 to 30 hpf as described earlier. At 30 hpf, embryos were transferred to clean, black 384-well microplates with 0.17-mm glass-bottom wells containing 50 µl of vehicle (0.2% DMSO) or 20 µM TPHP per well, and then exposed from 30 to 72 hpf as described earlier. This experimental design resulted in 48 embryos per treatment group and 4 different treatment groups per ligand. All 72-hpf embryos were anesthetized and imaged as described earlier.

HX 531 co-exposures

Based on results from the library screen, we used a pan-RXR antagonist (HX 531) to determine whether TPHP-induced cardiotoxicity was RXR-dependent. Using identical methods described earlier, the MTC for HX 531 was determined to be 5.24 µM based on static exposure from 24 to 72 hpf. Therefore, we co-exposed embryos to TPHP (5, 10, or 20 µM) in the presence or absence of 2.62 or 5.24 µM HX 531 (0.5× and 1× MTC, respectively), and all 72-hpf embryos were anesthetized and imaged as described earlier.

Quantification of embryonic doses of TPHP and DPHP

To ensure that ciglitazone and/or fenretinide were not interfering with embryonic uptake or metabolism of TPHP, we quantified embryonic doses of TPHP and DPHP following co-exposure to ciglitazone or fenretinide in the presence or absence of TPHP. Briefly, 24-hpf embryos (30 embryos per dish; 3 dishes per treatment group) were placed into clear petri dishes containing 10 ml of vehicle (0.2% DMSO), 2.14 μM fenretinide, or 5.24 μM ciglitazone in the presence or absence of 20 μM TPHP. Embryos were incubated as described earlier until 72 hpf. For each replicate pool (3 pools per treatment), 30 72-hpf embryos were placed into a 2-ml cryovial, immediately snap-frozen in liquid nitrogen, and stored at −80°C until analysis. Immediately prior to extraction, samples were spiked with deuterated TPHP (d15-TPHP) and deuterated DPHP (d10-DPHP). Analytes were extracted and quantified similar to previously published methods (Isales *et al*., 2015). Tissue extracts were analyzed by LC/MS-MS on an Agilent 1260 Infinity II series LC connected to an Agilent 6460 A triple quadrupole MS detector equipped with an electrospray ionization source. Analytes were separated on a Luna C18 (2)-HST column (50 × 2 mm; 2.5 μm; Phenomenex, Torrance, California) maintained at 35°C. Method detection limits (MDLs) were defined as 3 times the standard deviation of lab blanks (if present) or 3 times the noise. MDLs for TPHP and DPHP were 0.45 and 0.1 ng, respectively.

Human RXR reporter assays

A cell-based human RXR-driven luciferase reporter assay developed by the Services Group within INDIGO Biosciences (State College, Pennsylvania) was used to determine whether TPHP was an agonist or antagonist of human RXRα-, RXRβ-, and/or RXRγ. 9-*cis*-retinoic acid (9-*cis*-RA) and 3-[4-Hydroxy-3-[5, 6, 7, 8-tetrahydro-5, 5, 8, 8-tetramethyl-3-(pentyloxy)-2-naphthalenyl]phenyl]-2-propenoic acid (UVI 3003) were used as a reference agonist and antagonist, respectively, for all 3 RXRs. Concentrated TPHP stock (50 mM) was serially diluted in DMSO to yield 3.1, 6.3, 13, and 25 mM stocks; concentrated 9-*cis*-RA stock was serially diluted in DMSO to yield 0.000061, 0.00032, 0.0016, 0.008, 0.040, 0.20, 1, and 5 mM stocks; and concentrated UVI3003 stock was serially diluted in DMSO to yield 0.00061, 0.0024, 0.01, 0.039, 0.156, 0.625, 2.5, and 10 mM stocks. Treatment solutions were prepared by diluting stocks in INDIGO's proprietary culture media, resulting in 0.1% DMSO within all wells. For agonist mode assays, treatment wells contained either vehicle (0.1% DMSO), 9-*cis*-RA (0.000061, 0.00032, 0.0016, 0.008, 0.040, 0.20, 1, and 5 μM), or TPHP (3.1, 6.3, 13, 25, or 50 μM). For antagonist mode assays, plates contained positive control wells containing 9-*cis*-RA that increased luminescence by approximately 80% relative to negative control wells. Treatment wells contained identical 9-*cis*-RA concentrations as positive control wells, but also contained TPHP (3.1, 6.3, 13, 25, or 50 μM) or UVI 3003 (0.0006, 0.002, 0.01, 0.04, 0.16, 0.63, 2.5, or 10 μM).

For each treatment group, spiked culture media (100 µl) was dispensed into triplicate assay wells (using a white 96-well microplate) containing Chinese hamster ovary (CHO) cells stably transfected with (1) expression vector containing the N-terminal GAL4 DNA binding domain fused to the ligand-binding domain of human RXRα-, RXRβ-, or RXRγ and (2) reporter vector containing a firefly luciferase gene functionally linked to the GAL4-specific upstream activation sequence. Following a 24-h incubation at 37°C under 5% carbon dioxide (CO_2), treatment media was discarded and, following 1 rinse with INDIGO's proprietary live cell multiplex buffer, live cell multiplex substrate was added to each well of the assay plate to assess cell viability. Following incubation at 37°C for 30 min, fluorescence was quantified to determine the relative number of live cells per well, and then live cell multiplex substrate was discarded and 100 µl of ONE-Glo Luciferase Assay Reagent (Promega) was added to each well of the assay plate. After a 5-min incubation at room temperature, luminescence was quantified using a GloMax 96 microplate luminometer (Promega). Mean fluorescence and luminescence (± SD) values were calculated for each treatment group based on triplicate wells per treatment. For cell viability data, mean fluorescence for each treatment group was normalized to mean fluorescence for 9-*cis*-RA-only wells to determine the percent change in cell viability relative to positive control wells.

Statistical analyses

For exposure, analytical chemistry, and human RXR assay data, a general linear model (GLM) analysis of variance (ANOVA) ($\alpha = 0.05$) was performed using SPSS Statistics 24, as these data did not meet the equal variance assumption for nonGLM ANOVAs. Treatments groups were compared with vehicle controls using pair-wise Tukey-based multiple comparisons of least square means to identify significant differences in effects.

RESULTS

TPHP Induces Cardiotoxicity Following Initiation of Exposure at 24 hpf

Although survival was >85% across all treatment groups, exposure to TPHP from 24 to 72 hpf resulted in (1) a significant, concentration-dependent decrease in percent hatch starting at 25.6 µM TPHP (Supplementary Figure 1A); (2) a significant, concentration-dependent decrease in body length starting at 16.4 µM TPHP (Supplementary Figure 1B); and (3) a significant, concentration-dependent increase in pericardial area starting at 8.4 µM TPHP (Supplementary Figure 1C). These data are consistent with our previous results based on exposures from 5 to 72 hpf within 384-well plates (Isales *et al*., 2015). Therefore, we selected 20-µM TPHP as an optimal concentration for all coexposures and pretreatment experiments, as this TPHP concentration reliably induced cardiotoxicity based on a 24- to 72-hpf exposure.

mRNA Sequencing Reveals That TPHP Disrupts RXR-Dependent Pathways

Raw DESeq2 output for 5, 10, and 20 µM TPHP are provided within Supplementary Tables 2–4, respectively. Based on these data, TPHP exposure from 24 to 72 hpf resulted in a concentration-dependent increase in the total number, magnitude, and statistical significance of affected transcripts at 72 hpf relative to vehicle (0.2% DMSO) controls (Figs. 1A–C for 5, 10, and 20 µM TPHP, respectively). Moreover, there was a concentration-dependent increase in the proportion of significantly decreased transcripts (relative to the total number of significantly affected transcripts), where 0% (0 out of 13), 32% (16 out of 50),

and 49% (148 out of 302) of transcripts were decreased following exposure to 5, 10, or 20 µM TPHP, respectively. Based on the lowest *p*-adjusted value, the most significantly affected transcripts following exposure to 5, 10, or 20 µM TPHP were *titin-cap (tcap*), *rhodopsin* (*rho*), and *MAP kinase interacting serine/threonine kinase 2 b* (*mknk2b*), respectively (Supplementary Tables 2–4).

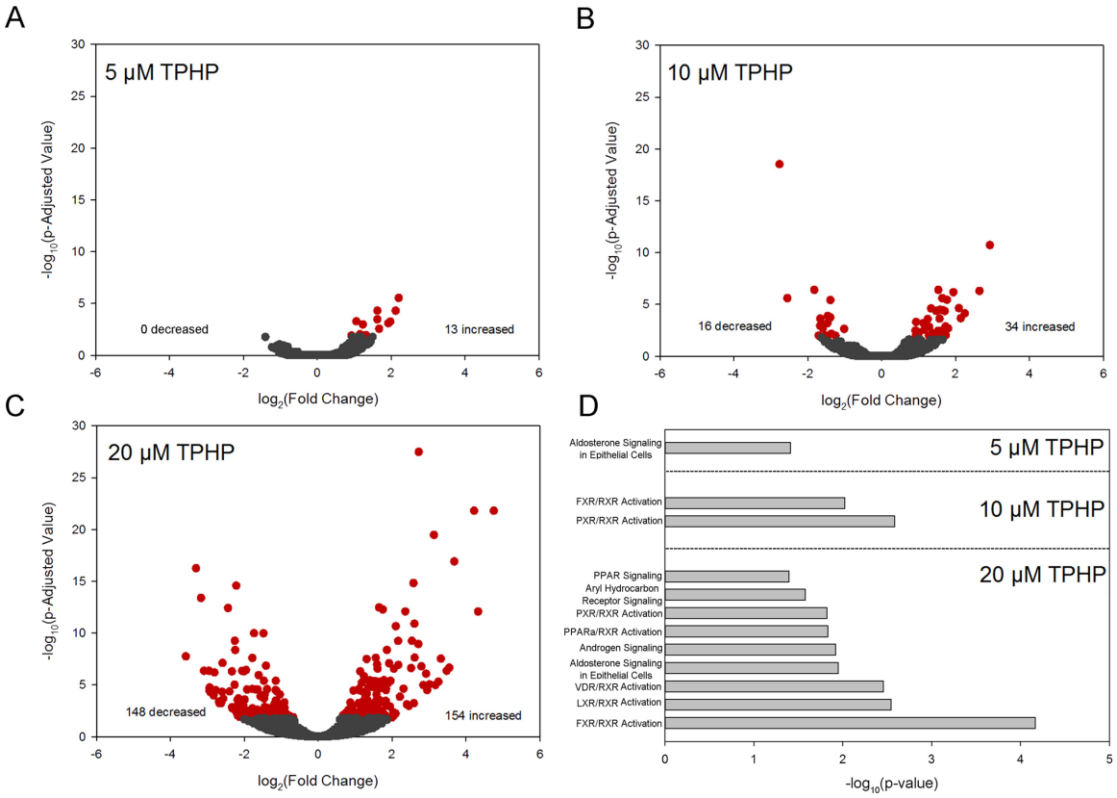

Figure 1. Volcano plots showing the number of significantly different transcripts (red circles) within 5, 10, and 20 µM TPHP (A–C), with the log_2-transformed fold change plotted on the x-axis and the log_{10}-transformed *p*-adjusted value on the y-axis. Nuclear receptor pathways (D) affected by TPHP were identified by IPA's Tox-Analysis using a Fisher's exact *p*-value ≤ .05, with 6 nuclear receptors containing RXR as a heterodimer.

Curated data available within the Zebrafish Information Network (https://zfin.org/) were then queried to identify wildtype embryonic tissues that normally express transcripts that were significantly impacted in our study. Based on this analysis, we found that 23% (3 out of 13), 20% (10 out of 50), and 12% (36 out of 302) of transcripts following exposure to 5, 10, or 20 µM TPHP, respectively, have been detected within the heart of wildtype embryos (Supplementary Tables 2–4). Interestingly, *tcap*, *fatty acid-binding protein 1b, tandem duplicate 1* (*fabp1b.1*), and *desmin a* (*desma*)—all 3 of which are expressed within the heart—were significantly increased following exposure to 5 and 10 µM TPHP. Moreover, *desma* was significantly increased following exposure to all 3 TPHP concentrations, suggesting that this transcript may be a potential indicator of TPHP-induced cardiotoxicity within zebrafish.

Following automated identification of human, rat, or mouse homologs within IPA, 38% (5 out of 13), 50% (25 out of 50), and 58% (175 out of 302) of statistically significant transcripts within embryos exposed to 5, 10, and 20 µM TPHP, respectively, were included in IPA's Tox Analysis; the remaining statistically significant transcripts were excluded by IPA's Tox Analysis due to the absence of human, rat, and/or mouse orthologs within NCBI's Homologene database. A complete list of all significantly affected canonical pathways identified by IPA's Tox Analysis for 5, 10, and 20 µM TPHP are provided within Supplementary Tables 5–7, respectively. Interestingly, based on the remaining transcripts used within IPA, there was a concentration-dependent increase in the number of

significantly affected cardiovascular signaling pathways, where 2, 3, and 6 cardiovascular signaling pathways were impacted within embryos exposed to 5, 10, and 20 µM TPHP, respectively (Supplementary Tables 5–7).

In addition, transcripts linked to a total of 9 nuclear receptor signaling pathways were significantly affected following exposure to 5, 10, and/or 20 µM TPHP (Figure 1D). Interestingly, 5 of these 9 nuclear receptor signaling pathways were RXR-dependent, and there was a concentration-dependent increase in the number of RXR-dependent pathways affected by TPHP. Although aldosterone signaling in epithelial cells represented a significantly impacted nuclear receptor signaling pathway within embryos exposed to 5 and 20 µM TPHP, this pathway was not significant at 10 µM TPHP due to a lack of significant differences in the abundance of *HSPA1L* (a heat shock gene)—a transcript that was significantly increased within embryos exposed to 5 and 20 µM TPHP.

Fifteen Out of Seventy-Four Nuclear Receptor Ligands Mitigate TPHP-Induced Cardiotoxicity Following Coexposure From 24 to 72 hpf

Our nuclear receptor library screen identified the following 15 out of 74 nuclear receptor ligands that, compared with embryos treated with 20 µM TPHP alone, significantly and reliably decreased TPHP-induced pericardial area (Figure 2; Supplementary Tables 8 and 9): 4-hydroxyretinoic acid (retinoid metabolite), 9-*cis*RA (a RXR agonist), 13-*cis* RA (RAR agonist), 24(S)-hydroxycholesterol (a liver X receptor, or LXR, agonist), acitretin (retinoid),

adapalene (RA analog), bisphenol A diglycidyl ether (PPARγ antagonist), ciglitazone (PPARγ agonist), clofibric acid (PPARα agonist), fenretinide (RAR agonist), geranylgeraniol (farnesoid), LY 171883 (PPARγ agonist), pregnenolone (progesterone precursor), TTNPB (RAR agonist), and WY-14643 (PPAR agonist). We screened all 15 ligands in concentration-response format as described earlier, and found that 2 ligands (ciglitazone and fenretinide) reproducibly decreased TPHP-induced cardiotoxicity in a concentration-dependent manner (Figure 3; Supplementary Table 10).

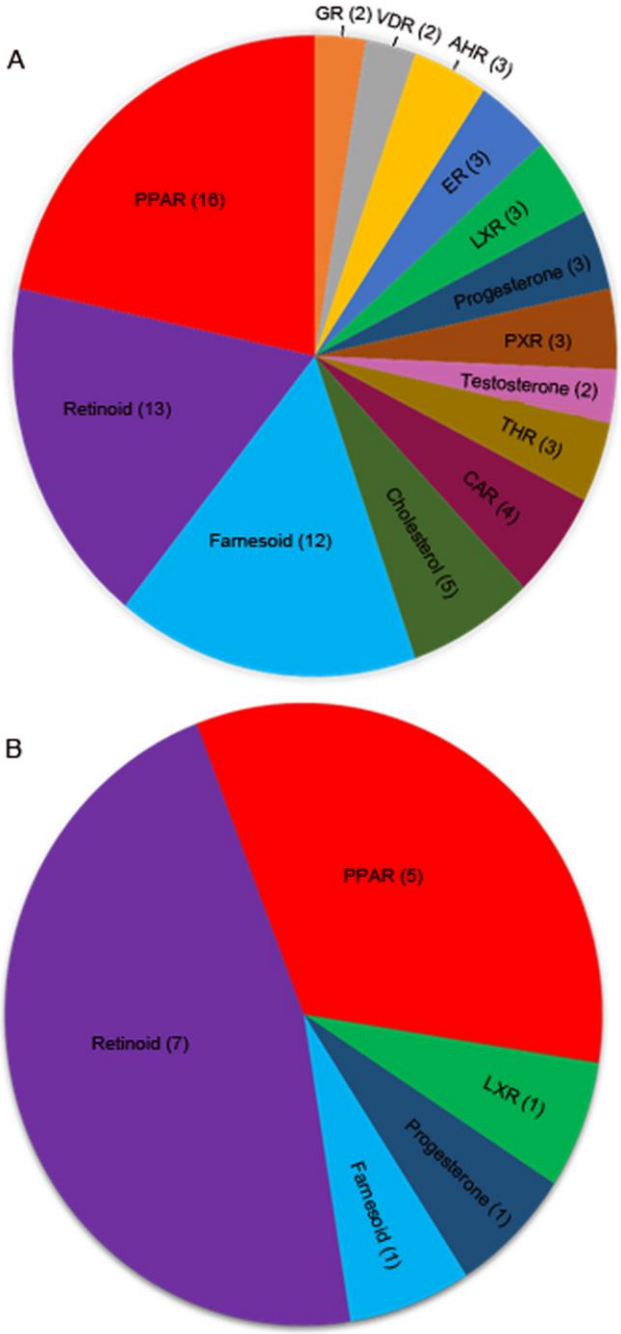

Figure 2. Distribution of ligands by target nuclear receptor for the entire SCREEN-WELL Nuclear Receptor ligand library (A), and 15 ligands that mitigated TPHP-induced cardiotoxicity following co-exposure from 24 to 72 hpf (B). Number in parenthesis denotes number of ligands per target nuclear receptor.

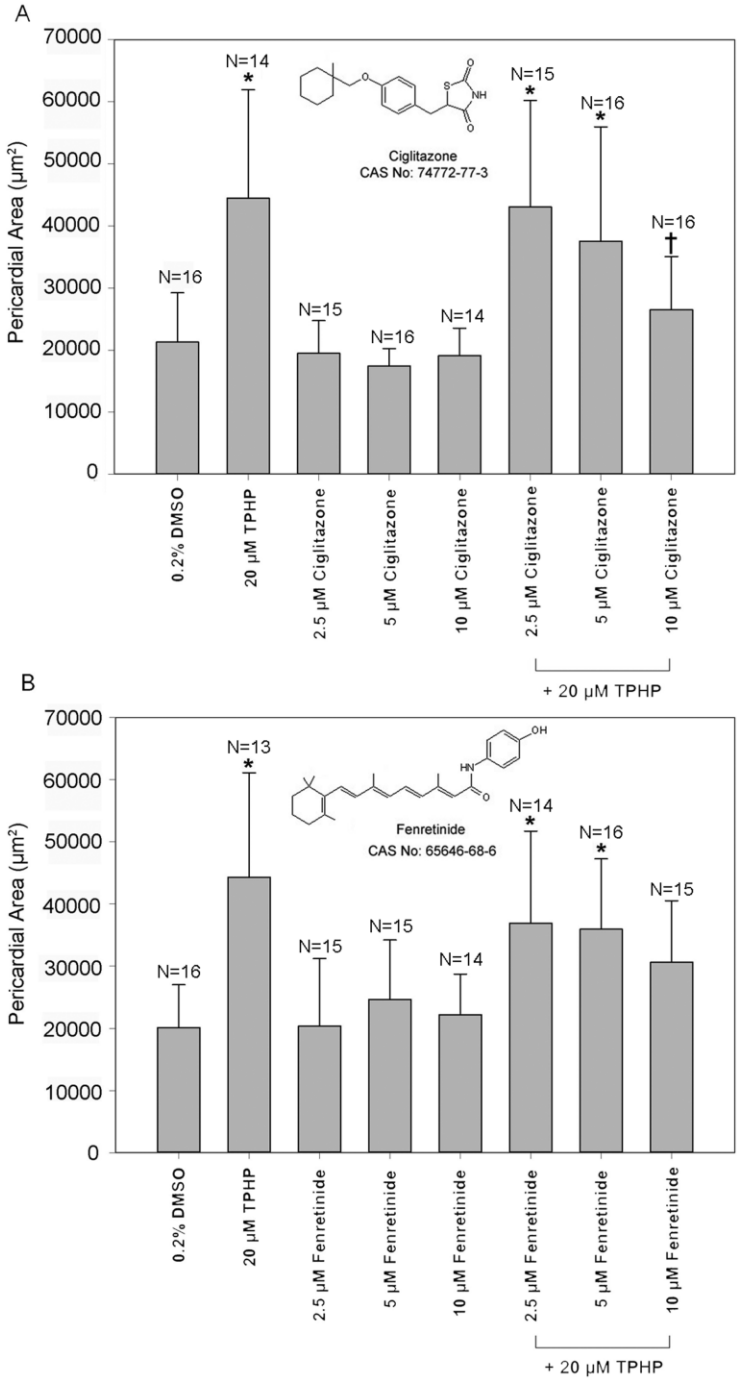
A
Pericardial Area (µm²)
70000
60000
50000
40000
30000
20000
10000
0
N=16
N=14
N=15
N=16
N=14
N=15
N=16
N=16
Ciglitazone
CAS No: 74772-77-3
0.2% DMSO
20 µM TPHP
2.5 µM Ciglitazone
5 µM Ciglitazone
10 µM Ciglitazone
2.5 µM Ciglitazone
5 µM Ciglitazone
10 µM Ciglitazone
+ 20 µM TPHP
B
Pericardial Area (µm²)
70000
60000
50000
40000
30000
20000
10000
0
N=16
N=13
N=15
N=15
N=14
N=14
N=16
N=15
Fenretinide
CAS No: 65646-68-6
0.2% DMSO
20 µM TPHP
2.5 µM Fenretinide
5 µM Fenretinide
10 µM Fenretinide
2.5 µM Fenretinide
5 µM Fenretinide
10 µM Fenretinide
+ 20 µM TPHP

Figure 3. Mean pericardial area (± SD) for 72-hpf embryos treated with vehicle (0.2% DMSO) or ciglitazone (2.5, 5, or 10 µM) in the presence or absence of 20 µM TPHP from 24 to 72 hpf (A). Mean pericardial area (± SD) for 72-hpf embryos treated with vehicle (0.2% DMSO) or fenretinide (2.5, 5, or 10 µM) in the presence or absence of 20 µM TPHP from 24 to 72 hpf (B). Asterisk (*) denotes significant treatment effect ($p < .05$) relative to vehicle controls (0.2% DMSO), whereas single cross (†) denotes significant co-exposure effect ($p < .05$) relative to embryos exposed to 20 µM TPHP alone (*n*, final number of embryos analyzed per treatment).

Pretreatment with Ciglitazone or Fenretinide Mitigates TPHP-Induced Cardiotoxicity

To ensure that ciglitazone and fenretinide were not interfering with embryonic TPHP uptake nor interacting with TPHP in solution, we pretreated embryos with MTCs of ciglitazone or fenretinide (based on survival, hatch, body length, or pericardial area) from 24 to 30 hpf, followed by treatment with 20 μM TPHP alone from 30 to 72 hpf. Based on these experiments, we found that pretreatment with ciglitazone or fenretinide significantly mitigated TPHP-induced cardiotoxicity, although these 2 ligands were unable to block TPHP-induced effects on body length (Figure 4).

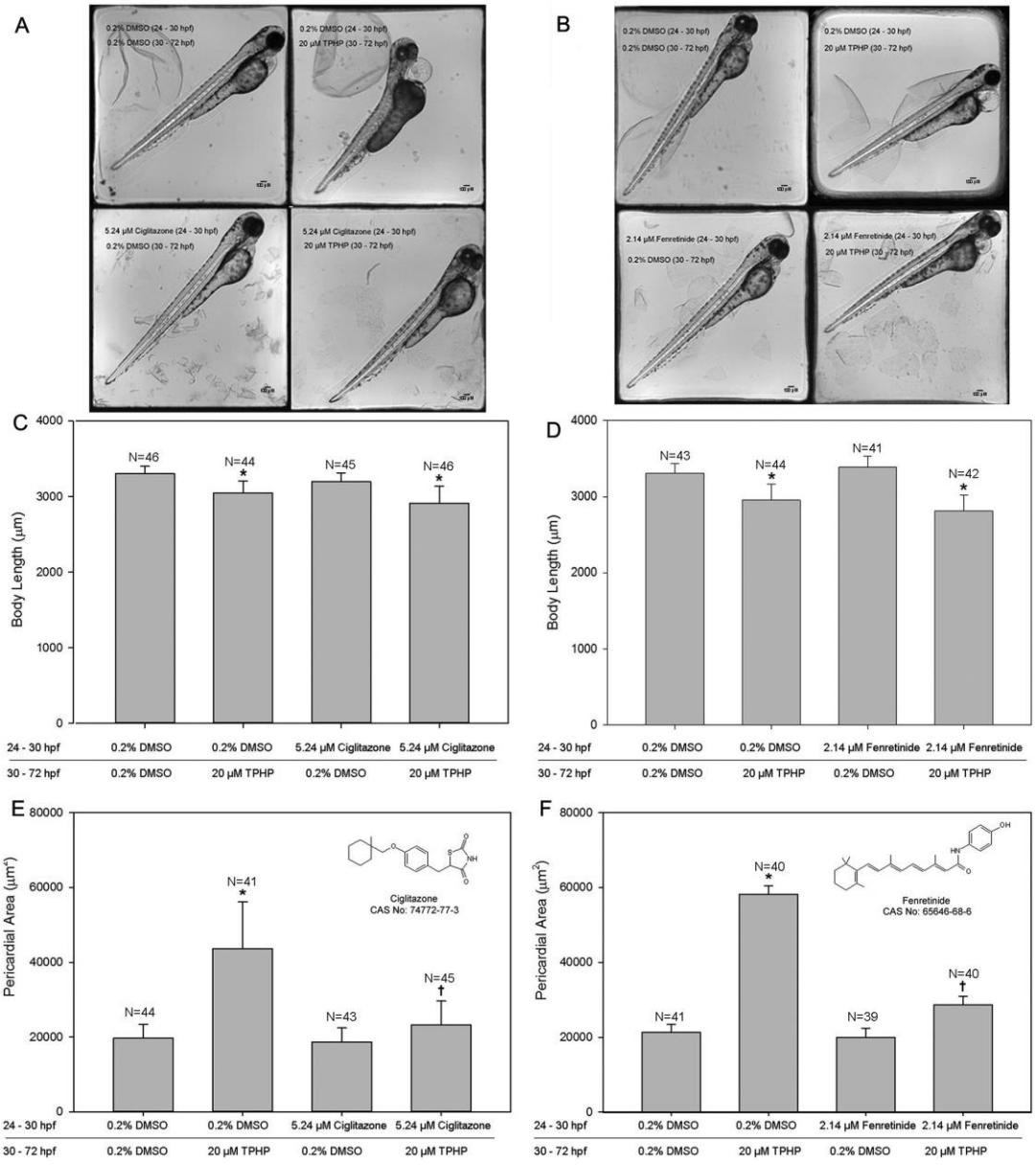
A
0.2% DMSO (24 - 30 hpf)
0.2% DMSO (30 - 72 hpf)
0.2% DMSO (24 - 30 hpf)
20 µM TPHP (30 - 72 hpf)
5.24 µM Ciglitazone (24 - 30 hpf)
0.2% DMSO (30 - 72 hpf)
5.24 µM Ciglitazone (24 - 30 hpf)
20 µM TPHP (30 - 72 hpf)
B
0.2% DMSO (24 - 30 hpf)
0.2% DMSO (30 - 72 hpf)
0.2% DMSO (24 - 30 hpf)
20 µM TPHP (30 - 72 hpf)
2.14 µM Fenretinide (24 - 30 hpf)
0.2% DMSO (30 - 72 hpf)
2.14 µM Fenretinide (24 - 30 hpf)
20 µM TPHP (30 - 72 hpf)
C
Body Length (µm)
N=46
N=44
N=45
N=46
D
Body Length (µm)
N=43
N=44
N=41
N=42
24 - 30 hpf
30 - 72 hpf
0.2% DMSO
0.2% DMSO
0.2% DMSO
20 µM TPHP
5.24 µM Ciglitazone
0.2% DMSO
5.24 µM Ciglitazone
20 µM TPHP
2.14 µM Fenretinide
0.2% DMSO
2.14 µM Fenretinide
20 µM TPHP
E
Pericardial Area (µm²)
Ciglitazone
CAS No: 74772-77-3
N=44
N=41
N=43
N=45
F
Pericardial Area (µm²)
Fenretinide
CAS No: 65646-68-6
N=41
N=40
N=39
N=40

Figure 4. Representative images (A, B)**,** mean body length (± SD) (C, D), and mean pericardial area (± SD) (E, F) of 72-hpf embryos pretreated with vehicle (0.2% DMSO), 5.24 µM ciglitazone, and 2.14 µM fenritinide from 24 to 30 hpf, and then treated with vehicle (0.1% DMSO) or 20 µM TPHP from 30 to 72 hpf. Images were acquired using a 4× objective and transmitted light within our ImageXpress Micro XLS Widefield High-Content Screening System. Asterisk (*) denotes significant treatment effect ($p < .05$) relative to vehicle controls (0.2% DMSO), whereas single cross (†) denotes significant pretreatment effect ($p < .05$) relative to embryos exposed to 20 µM TPHP alone (*n*, final number of embryos analyzed per treatment).

Co-exposure With Ciglitazone or Fenretinide Does Not Affect Embryonic Doses of TPHP or DPHP

Mean embryonic doses of TPHP following a 24- to 72-hpf exposure to vehicle (0.2% DMSO), 5.24 µM ciglitazone, or 2.14 µM fenretinide were below the MDL, whereas mean embryonic doses of TPHP following a 24- to 72-hpf exposure to 20 µM TPHP, 20 µM TPHP + 5.24 µM ciglitazone, or 20 µM TPHP + 2.14 µM fenretinide were 3982, 3423, and 4947 ng per 30 embryos, respectively (Supplementary Figure 2). Mean embryonic doses of DPHP were <29 ng per 30 embryos across all treatments.

Co-exposure to a pan-RXR Antagonist (HX 531) From 24 to 72 hpf Enhances TPHP-Induced Cardiotoxicity

As RXR antagonists were absent from the SCREEN-WELL Nuclear Receptor Ligand Library and our results with fenretinide (a pan-RAR agonist) and ciglitazone (a PPARγ agonist) suggested that TPHP may activate RXR (a heterodimer for both RARs and PPARγ), we co-exposed embryos from 24 to 72 hpf to vehicle (0.2% DMSO) or TPHP (5, 10, or 20 µM) in the presence or absence of HX 531 (2.62 or 5.24 µM), a pan-RXR antagonist. However, contrary to our hypothesis, we found that coexposure to 20 µM TPHP and 5.24 µM HX 531 resulted in a significant increase in pericardial area relative to embryos exposed to 20 µM TPHP (Figure 5).

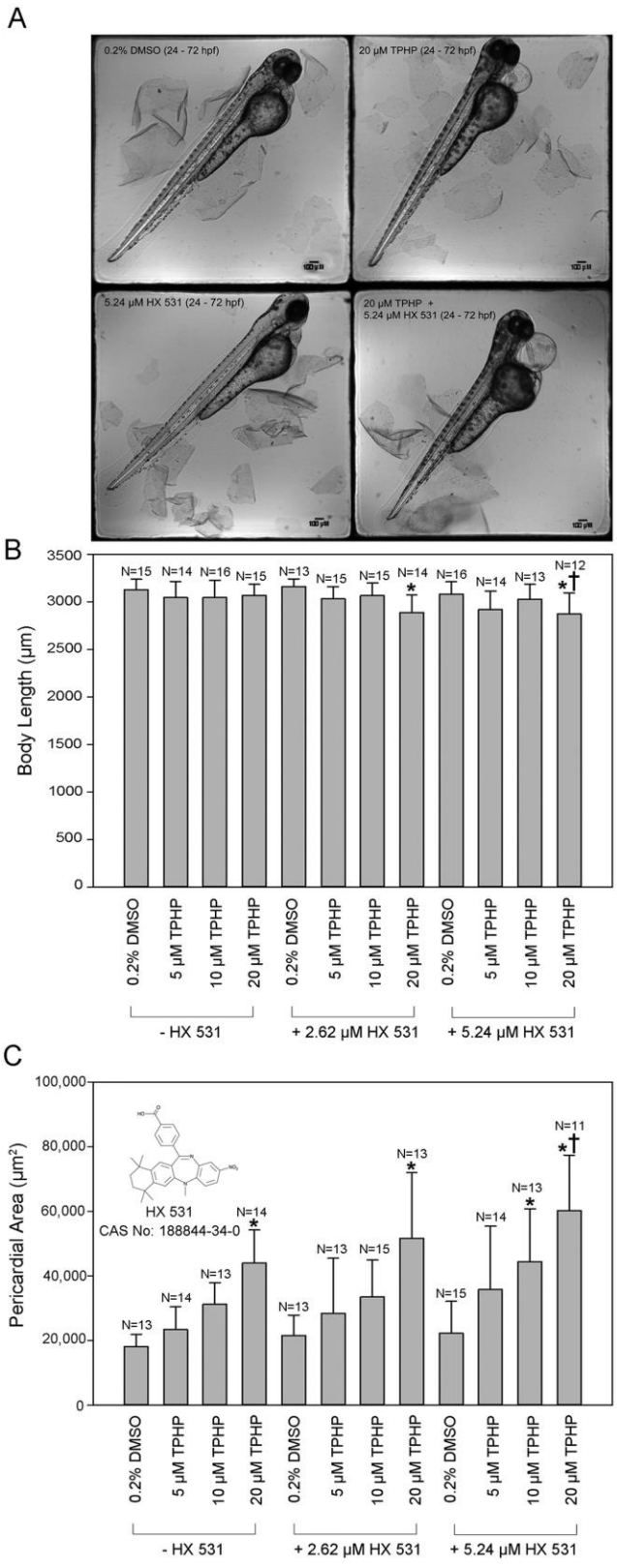
A
0.2% DMSO (24 - 72 hpf)
20 µM TPHP (24 - 72 hpf)
5.24 µM HX 531 (24 - 72 hpf)
20 µM TPHP +
5.24 µM HX 531 (24 - 72 hpf)
B
Body Length (µm)
3500
3000
2500
2000
1500
1000
500
0
N=15 N=14 N=16 N=15 N=13 N=15 N=15 N=14 N=16 N=14 N=13 N=12
0.2% DMSO
5 µM TPHP
10 µM TPHP
20 µM TPHP
- HX 531
+ 2.62 µM HX 531
+ 5.24 µM HX 531
C
Pericardial Area (µm²)
100,000
80,000
60,000
40,000
20,000
0
HX 531
CAS No: 188844-34-0
N=13 N=14 N=13 N=14 N=13 N=13 N=15 N=13 N=15 N=14 N=13 N=11

Figure 5. Representative images (A)**,** mean body length (± SD) (B), and mean pericardial area (± SD) (C) of 72-hpf embryos coexposed to vehicle (0.2% DMSO) or HX 531 (2.62 or 5.24 µM) in the presence or absence of 20 µM TPHP from 24 to 72 hpf. Asterisk (*) denotes significant treatment effect ($p < .05$) relative to vehicle controls (0.2% DMSO), whereas single cross (†) denotes significant co-exposure effect ($p < .05$) relative to embryos exposed to 20 µM TPHP alone (*n*, final number of embryos analyzed per treatment).

TPHP Is Not an Agonist nor Antagonist of Human RXRα-, RXRβ-, or RXRγ Within CHO Cells

Although 9-*cis*-RA was a potent agonist for all 3 human RXRs, TPHP did not activate human RXRs at any of the concentrations tested (up to 50 µM) (Figure 6)**.** Similarly, compared with UVI 3003 (a RXR antagonist), exposure to TPHP at all concentrations tested (up to 50 µM) resulted in no effect on 9-*cis*-RA-induced activation of human RXRα-, RXRβ-, or RXRγ (Figure 6). Cell viability (percent live cells) was >89% across all 3 assays for UVI 3003, 9-*cis*-RA and TPHP exposures (Supplementary Tables 11 and 12).

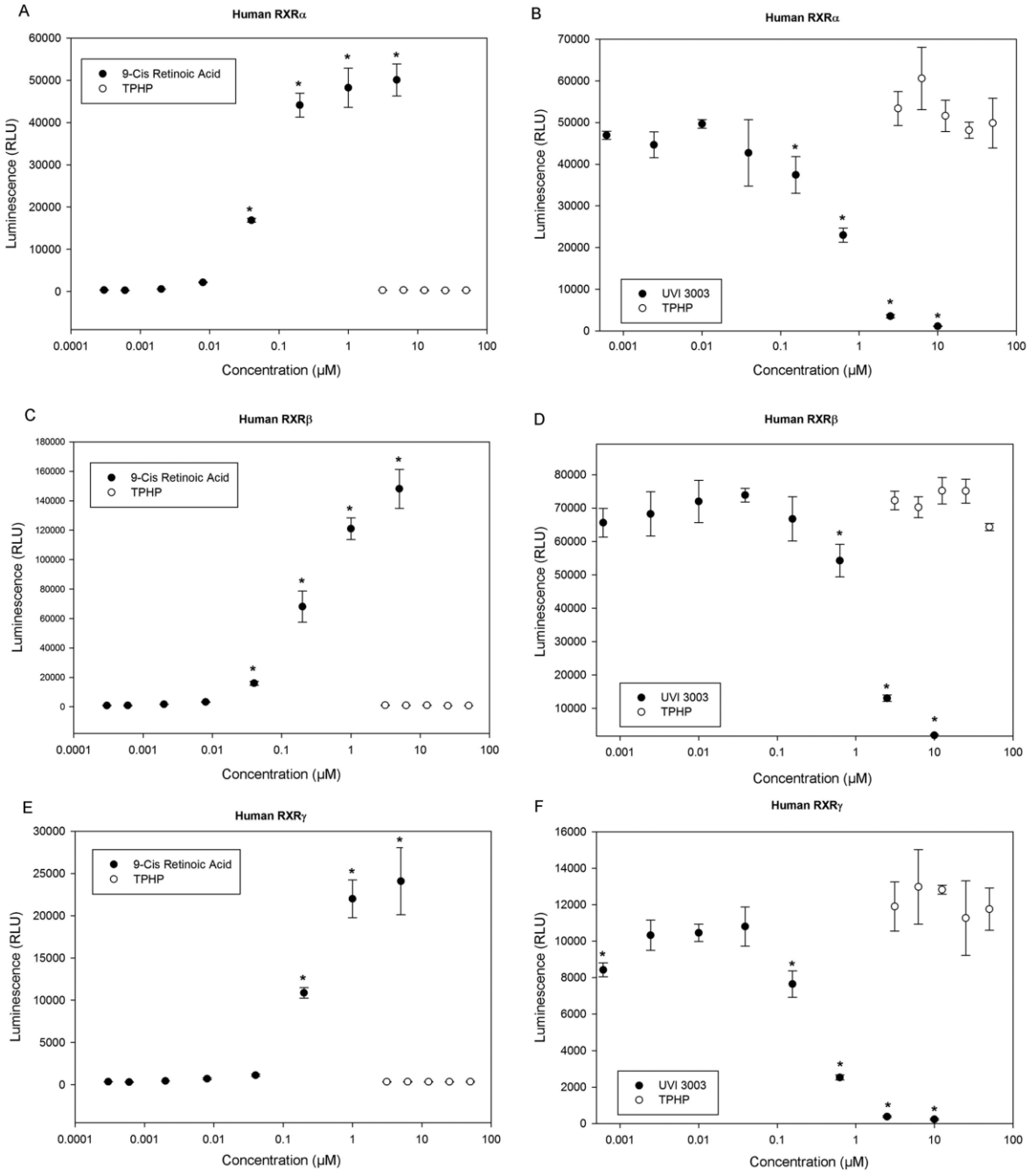
A
Human RXRα
9-Cis Retinoic Acid
TPHP
Luminescence (RLU)
Concentration (μM)
B
Human RXRα
UVI 3003
TPHP
Luminescence (RLU)
Concentration (μM)
C
Human RXRβ
9-Cis Retinoic Acid
TPHP
Luminescence (RLU)
Concentration (μM)
D
Human RXRβ
UVI 3003
TPHP
Luminescence (RLU)
Concentration (μM)
E
Human RXRγ
9-Cis Retinoic Acid
TPHP
Luminescence (RLU)
Concentration (μM)
F
Human RXRγ
UVI 3003
TPHP
Luminescence (RLU)
Concentration (μM)

Figure 6. Mean luminescence (± SD) from human RXRα- (A, B), RXRβ- (C, D), and RXRγ-expressing (E, F) CHO cells following exposure to 9-*cis*-retinoic acid (reference RXRα agonist), UVI 3003 (reference RXRα antagonist), or TPHP in agonist (A, C, E) or antagonist (B, D, F) mode. Asterisk (*) denotes significant treatment effect ($p < .05$) relative to vehicle controls (0.1% DMSO).

DISCUSSION

Although TPHP exposure is ubiquitous and has been detected in urine samples (Ospina *et al*., 2018), surface water (Kim *et al*., 2017), and indoor environments (Castorina *et al*., 2017), little is known about the potential effects of TPHP on early development within humans and wildlife. Within this study, we showed that, similar to initiation of exposure at 5 hpf (approximately 50% epiboly) (Isales *et al*., 2015), TPHP disrupted cardiac development following initiation of exposure at 24 hpf (Prim-5), demonstrating that the sensitive window for TPHP exposure in zebrafish was the pharyngula period (24–48 hpf)—a developmental window that includes cardiac looping—and not earlier embryonic stages (<24 hpf) that include differentiation and migration of cardiac progenitor cells. Similar to TPHP, other well-studied environmental chemicals such as 2,3,7,8-tetrachlorodibenzo-*p*-dioxin (TCDD) (Antkiewicz et al., 2005; Henry *et al*., 1997) and phenanthrene (Zhang *et al.,*2013) disrupt heart morphogenesis during zebrafish development, resulting in cardiotoxicity during pharyngula. Within zebrafish, initiation of TCDD exposure at either 5 or 24 hpf resulted in a similar magnitude of effect later in development (based on cardiotoxicity and lethality), whereas initiation of TCDD exposure after cardiac formation results in decreased sensitivity and toxicity (Lanham *et al.,* 2012). Similarly, initiation of exposure to phenanthrene at 6 hpf resulted in a decrease in blood circulation at 36 hpf and increase in pericardial edema at 48 hpf (Incardona *et al*. 2004), suggesting that, similar to TCDD, pharyngula represents the sensitive window of exposure for phenanthrene.

Similar to these persistent organic compounds, our data support the hypothesis that TPHP interferes with developmental pathways involved in cardiac looping and chamber formation rather than tube heart assembly.

TPHP-induced effects on cardiac tissue were also supported by our mRNA-seq data, as *desmin* was significantly increased relative to vehicle controls following exposure to all 3 TPHP concentrations. Desmin is a muscle-specific intermediate filament protein that is localized to z-discs within cardiac, skeletal, and smooth muscles (Paulin and Li, 2004). Importantly, Desmin proteins play a major role in the maintenance and integrity of muscle tissue by forming a 3D scaffold that serves as a bridge from z-discs to other key muscle components (Paulin and Li, 2004). In zebrafish, *desmin* is expressed as early as the 1- to 3-somite stage, with maximum expression occurring during Prim-6 (approximately 25 hpf) (Loh *et al.,* 2000). After expression declines from 25 to 72 hpf, *desmin* is primarily localized to muscles throughout the developing embryo (Loh *et al.,* 2000). In zebrafish, morpholino knockdown of *desmin* leads to decreased sarcomere units, widened and misaligned z-discs, and cardiac defects at 72 hpf, including cardiac edema, disorganized muscle structure, and aberrant cardiac looping (Vogel *et al.,* 2009; Li *et al.,* 2013). Although overexpression and altered distribution of *desmin* are observed in human hearts with end-stage congestive heart failure (Heling *et al.,* 2002), overexpression of *desmin* in mice display no apparent cardiac deformities nor shortened life spans (Wang *et al.,*2002). Therefore,

similar to humans, increased levels of *desmin* at 72 hpf in zebrafish may be an indicator of heart failure following TPHP exposure.

We previously showed that TPHP disrupts RAR-dependent pathways (Isales *et al*., 2015), although it is unknown if this interaction is direct or indirect. Therefore, in this study, we relied on IPA to investigate potential nuclear receptor pathways involved in TPHP-induced cardiotoxicity in zebrafish. Interestingly, based on our mRNA-sequencing data, IPA's Tox Analysis revealed that 5 out of 9 nuclear receptor pathways that were significantly impacted were RXR-dependent, suggesting that RXR may be a central mediator of TPHP-induced cardiotoxicity. Other studies have evaluated the role of RXR in cardiac development within vertebrates. For example, exposure of zebrafish embryos to a pan-RXR antagonist (UVI3003) resulted in a wide range of malformations (including cardiac defects) and, similar to our findings with TPHP, pharyngula (24–48 hpf) was the most sensitive window for UVI3003-induced toxicity (Zheng *et al.,* 2015). Moreover, studies in mice have shown that RARα/RXRα is the predominant heterodimer pair involved in RA-induced myocardial growth and cardiac development (Mascrez *et al.*, 1998), and that RXRα promotes binding to response elements following RA-induced RARα activation (Mic *et al*., 2003). This is contrary to RXR-specific heterodimerization with other nuclear receptors such as PPARs, where RXR may mediate transcription in addition to RXR's heterodimer partners (DiRenzo *et al.,* 1997). Therefore, the presence of multiple heterodimer partners for RXR, combined with stage- and tissue-dependent roles

in transcription, underscores the complexity of RXR-dependent signaling and challenges of uncovering 1 or more mechanisms of action for environmentally-relevant chemicals such as TPHP.

Based on results from our nuclear receptor ligand library screen and follow-up experiments, ciglitazone (a PPARγ agonist) and fenretinide (RAR agonist) reliably decreased pericardial edema (a biomarker for cardiac looping defects) in a concentration-dependent manner. While we did not assess the affinity of these ligands to zebrafish-specific RARs and PPARγ, both compounds are potent RAR and PPARγ agonists in human cells (Lee *et al*., 2012; Pergolizzi *et al*., 1999). As PPARγ- and RAR-dependent signaling are necessary for cardiac development (Barak *et al.,* 1999; Li *et al.,* 2016) and pretreatment with either ciglitazone or fenretinide blocked TPHP-induced cardiotoxicity, our findings suggest that TPHP may disrupt normal PPARγ- and RAR-dependent signaling required for proper heart development. Moreover, neither embryonic uptake nor metabolism of TPHP was influenced by co-exposure to ciglitazone or fenretinide, demonstrating that ciglitazone and fenretinide uptake interfered with TPHP's mechanism(s) of action responsible for cardiotoxicity during pharyngula (24–48 hpf). Overall, these data suggest that, similar to conclusions from our mRNA-sequencing data, TPHP may be interfering with RXR during cardiac looping, as RXR is a heterodimer for both RARs and PPARγ.

As these data suggested that TPHP may be activating RXR, we co-exposed embryos to HX 531—a pan-RXR antagonist—from 24 to 72 hpf and, contrary to

our hypothesis, found that coexposure to HX 531 significantly enhanced TPHP-induced cardiotoxicity. These findings support the conclusion that, similar to our findings with BMS493 (a pan-RAR antagonist) (Isales *et al.* 2015), TPHP may be acting as an RXR antagonist or indirectly decreasing RXR-dependent signaling. However, within our human RXR reporter assays, we found that TPHP was not an agonist or antagonist of human RXRα-, RXRβ-, or RXRγ within CHO cells, suggesting that TPHP may not directly bind to RXR within zebrafish. While we did not assess the affinity of HX 531 to zebrafish RXRs (6 genes total: *rxraa, rxrab, rxrba, rxrbb, rxrga,* and *rxrgb*) (Waxman and Yelon, 2007), other studies have confirmed that HX 531 is a potent RXR antagonist in human cells (Ebisawa *et al.,* 1999; Suzuki *et al.* 2009). However, as zebrafish do not possess RARβ (Waxman and Yelon, 2007), there may be differences in ligand-binding specificity and/or disruption of human versus zebrafish RXR signaling following exposure to RXR ligands. Moreover, our human RXR reporter assays only addressed direct interference at the receptor (RXR)-level, whereas our zebrafish assays addressed the potential for TPHP to indirectly interfere with RXR-dependent pathways via direct effects on upstream, RXR-connected pathways. For example, nuclear receptor subfamily 2, group F, member 2 (NR2F2) decreases RAR/RXR signaling by heterodimerizing with RXR (Cooney *et al.*, 1992; Tran *et al.*, 1992), and is essential for proper cardiac development in mice (Pereira *et al.*, 1999) and vascular development in zebrafish (Swift *et al.*, 2014; Wu *et al.*, 2014). Therefore, this raises the possibility that, within zebrafish,

TPHP may be directly activating NR2F2, resulting in increased NR2F2/RXR heterodimerization and altered RAR/RXR signaling.

In summary, our data collectively suggest that zebrafish nuclear receptors pathways—in particular RXR-dependent pathways—may be involved in mediating TPHP-induced cardiotoxicity. However, we recognize that additional research is needed to (1) determine whether TPHP is a ligand for zebrafish RXRs; (2) confirm that TPHP-induced toxicity in zebrafish embryos is RXR-dependent using genetic approaches that knockdown RXR function; and (3) better characterize TPHP-induced disruption of RXR-mediated signaling networks *in vivo*. Nevertheless, our current findings continue to highlight the complexity of deciphering mechanisms of developmental toxicity for TPHP in zebrafish and other animal models.

References

Antkiewicz D. S. , Burns C. G., Carney S. A., Peterson R. E., Heideman W. (2005). Heart malformation is an early response to TCDD in embryonic zebrafish. Toxicol. Sci . 84, 368–377.

Barak Y. , Nelson M. C., Ong E. S., Jones Y. Z., Ruiz-Lozano P., Chien K. R., Koder A., Evans R. M. (1999). PPAR gamma is required for placental, cardiac, and adipose tissue development. Mol. Cell 4, 585–595.

Basson C. T. , Bachinsky D. R., Lin R. C., Levi T., Elkins J. A., Soults J., Grayzel D., Kroumpouzou E., Traill T. A., Leblanc-Straceski J. (1997). Mutations in human TBX5 cause limb and cardiac malformation in Holt-Oram syndrome. Nat. Genet . 15, 30–35.

Belcher S. M. , Cookman C. J., Patisaul H. B., Stapleton H. M. (2014). In vitro assessment of human nuclear hormone receptor activity and cytotoxicity of the flame retardant mixture FM 550 and its triarylphosphate and brominated components. Toxicol. Lett . 228, 93–102.

Blumberg B. , Bolado J., Derguini F., Craig A. G., Moreno T. A., Chakravarti D., Heyman R. A., Buck J., Evans R. M. (1996). Novel retinoic acid receptor ligands in Xenopus embryos. Proc. Natl. Acad. Sci. U.S.A . 93, 4873–4878.

Brooke D. , Crookes M., Quarterman P., Burns J. (2009). Environmental Risk Evaluation Report: Triphenyl Phosphate (CAS no. 115-86-6). Environment Agency, Bristol, UK. p. 140.

Castorina R. , Butt C., Stapleton H. M., Avery D., Harley K. G., Holland N., Eskenazi B., Bradman A. (2017). Flame retardants and their metabolites in the homes and urine of pregnant women residing in California (the CHAMACOS cohort). Chemosphere 179, 159–166.

Chandler V. L. , Maler B. A., Yamamoto K. R. (1983). DNA sequences bound specifically by glucocorticoid receptor in vitro render a heterologous promoter hormone responsive in vivo. Cell 33, 489–499.

Chen J. , Carney S. A., Peterson R. E., Heideman W. (2008). Comparative genomics identifies genes mediating cardiotoxicity in the embryonic zebrafish heart. Physiol. Genomics 33, 148–158.

Cooney A. J. , Tsai S. Y., O'Malley B. W., Tsai M. J. (1992). Chicken ovalalbumin upstream promoter transcription factor (COUP-TF) dimer binds to different GGTCA response elements, allowing COUP-TF to repress hormonal induction of the vitamin D3, thyroid hormone and retinoic acid receptors. Mol. Cell Biol . 12, 4153–4163.

DiRenzo J. , Söderstrom M., Kurokawa R., Ogliastro M. H., Ricote M., Ingrey S., Hörlein A., Rosenfeld M. G., Glass C. K. (1997). Peroxisome proliferator-activated receptors and retinoic acid receptors differentially control the interactions of retinoid X receptor heterodimers with ligands, coactivators, and corepressors. Mol. Cell. Biol . 17, 2166–2176.

Ebisawa M. , Umemiya H., Ohta K., Fukasawa H., Kawachi E., Christoffel G., Gronemeyer H., Tsuji M., Hashimoto Y., Shudo K.et al. , (1999). Retinoid X receptor-antagonistic diazepinylbenzoic acids. Chem. Pharm. Bull . 47, 1778–1786.

Giguere V. , Ong E. S., Segui P., Evans R. M. (1987). Identification of a receptor for themorphogen retinoic acid. Nature 330, 624–629.

Heling A. , Zimmermann R., Kostin S., Maeno Y., Hein S., Devaux B., Bauer E., Klovekorn W. P., Schlepper M., Schaper W.et al. , (2002). Increased expression of cytoskeletal, linkage, and extracellular proteins in failing human myocardium. Circ. Res . 86, 846–853.

Henry T. R. , Spitsbergen J. M., Hornung M. W., Abnet C. C., Peterson R. E. (1997). Early life stage toxicity of 2, 3, 7, 8-tetrachlorodibenzo-p-dioxin in zebrafish (Danio rerio). Toxicol. Appl. Pharmacol . 142, 56–68.

Incardona J. P. , Collier T. K., Scholz N. L. (2004). Defects in cardiac function precede morphological abnormalities in fish embryos exposed to polycyclic aromatic hydrocarbons. Toxicol. Appl. Pharmacol . 196, 191–205.

Isales G. M. , Hipszer R. A., Raftery T. D., Chen A., Stapleton H. M., Volz D. C. (2015). Triphenyl phosphate-induced developmental toxicity in zebrafish: Potential role of the retinoic acid receptor. Aquat. Toxicol . 161, 221–230.

Kim U. J. , Oh J. K., Kannan K. (2017). Occurrence, removal, and environmental emission of organophosphate flame retardants/plasticizers in a wastewater treatment plant in New York State. Environ. Sci. Technol . 51, 7872–7880.

Kimmel C. B. , Ballard W. W., Kimmel S. R., Ullmann B., Schilling T. F. (1995). Stages of embryonic development of the zebrafish. Dev. Dyn. 203, 253–310.

Lanham K. A. , Peterson R. E., Heideman W. (2012). Sensitivity to dioxin decreases as zebrafish mature. Toxicol. Sci . 127, 360–370.

Lee M. W. , Kim D. S., Kim H. R., Kim H. J., Yang J. M., Ryu S., Noh Y. H., Lee S. H., Son M. H., Jung H. L.et al. , (2012). Cell death is induced by ciglitazone, a peroxisome proliferator-activated receptor γ (PPARγ) agonist, independently of PPARγ in human glioma cells. Biochem. Biophys. Res. Commun . 417, 552–557.

Li J. , Yue Y., Zhao Q. (2016). Retinoic acid signaling is essential for valvulogenesis by affecting endocardial cushions formation in zebrafish embryos. Zebrafish 13, 9–18.

Li M. , Andersson-Lendahl M., Sejersen T., Arner A. (2013). Knockdown of desmin in zebrafish larvae affects interfilament spacing and mechanical properties of skeletal muscles. J. Gen. Physiol . 141, 335–345.

Loh S. , Chan W., Gong Z., Lim T., Chua K. (2000). Characterization of zebrafish (Danio rerio) desmin cDNA: An early molecular marker of myogenesis. Differentiation 65, 247–254.

Mascrez B. , Mark M., Dierich A., Ghyselinck N. B., Kastner P., Chambon P. (1998). The RXRalpha ligand-dependent activation function 2 (AF-2) is important for mouse development. Development 125, 4691–4707.

McGee S. P. , Konstantinov A., Stapleton H. M., Volz D. C. (2013). Aryl phosphate esters within a major PentaBDE replacement product induce cardiotoxicity in developing zebrafish embryos: Potential role of the aryl hydrocarbon receptor. Toxicol. Sci . 133, 144–156.

McKnight G. S. , Palmiter R. D. (1979). Transcriptional regulation of the ovalbumin and conalbumin genes by steroid hormones in chick oviduct. J. Biol. Chem . 254, 9050–9058.

Mendelsohn C. , Lohnes D., Decimo D., Lufkin T., LeMeur M., Chambon P., Mark M. (1994). Function of the retinoic acid receptors (RARs) during development (II). Multiple abnormalities at various stages of organogenesis in RAR double mutants. Development 120, 2749–2771.

Mendelsohn E. , Hagopian A., Hoffman K., Butt C. M., Lorenzo A., Congleton J., Webster T. F., Stapleton H. M. (2016). Nail polish as a source of exposure to triphenyl phosphate. Environ. Int . 86, 45–51.

Merki E. , Zamora M., Raya A., Kawakami Y., Wang J., Zhang X., Burch J., Kubalak S. W., Kaliman P., Belmonte J. C. I.et al. , (2005). Epicardial retinoid X receptor α is required for myocardial growth and coronary artery formation. Proc. Natl. Acad. Sci. U.S.A . 102, 18455–18460.

Mic F. A. , Molotkov A., Benbrook D. M., Duester G. (2003). Retinoid activation of retinoic acid receptor but not retinoid X receptor is sufficient to rescue lethal defect in retinoic acid synthesis. Proc. Natl. Acad. Sci. U.S.A . 100, 7135–7140.

Minucci S. , Leid M., Toyama R., Saint-Jeannet J. P., Peterson V. J., Horn V., Ishmael J. E., Bhattacharyya N., Dey A., Dawid I. B.et al. , (1997). Retinoid X receptor (RXR) within the RXR-retinoic acid receptor heterodimer binds its ligand and enhances retinoid-dependent gene expression. Mol. Cell Biol . 17, 644–655.

Moorman A. , Webb S., Brown N. A., Lamers W., Anderson R. H. (2003). Development of the heart: (1) formation of the cardiac chambers and arterial trunks. Heart 89, 806–814.

Ospina M. , Jayatilaka N. K., Wong L. Y., Restrepo P., Calafat A. M. (2018). Exposure to organophosphate flame retardant chemicals in the U.S. general population: Data from the 2013-2014 National Health and Nutrition Examination Survey. Environ. Int . 110, 32–41.

PAULIN D. , LI Z. (2004). Desmin: A major intermediate filament protein essential for the structural integrity and function of muscle. Exp. Cell Res . 301, 1–7.

Paganelli A. , Gnazoo V., Acosta H., Lopez S. L., Carrasco A. E. (2010). Glyphosate-based herbicides produce teratogenic effects on vertebrates by impairing retinoic acid signaling. Chem. Res. Toxicol . 23, 1586–1595.

Pereira F. A. , Qiu Y., Zhou G., Tsai M.-J., Tsai S. Y. (1999). The orphan nuclear receptor COUP-TFII is required for angiogenesis and heart development. Genes Dev . 13, 1037–1049.

Pergolizzi R. , Appierto V., Crosti M., Cavadini E., Cleris L., Guffanti A., Formelli F. (1999). Role of retinoic acid receptor overexpression in sensitivity to fenretinide and tumorigenicity of human ovarian carcinoma cells. Int. J. Cancer 81, 829–834.

Pillai H. K. , Fang M., Beglov D., Kozakov D., Vajda S., Stapleton H. M., Webster T. F., Schlezinger J. J. (2014). Ligand binding and activation of PPARγ by Firemaster 550: Effects on adipogenesis and osteogenesis. Environ. Health Perspect . 112, 1225–1232.

Polak P. , Domany E. (2006). Alu elements contain many binding sites for transcription factors and may play a role in regulation of developmental processes. BMC Genom . 7, 133.

Rhinn M. , Dollé P. (2012). Retinoic acid signaling during development. Development 139, 843–858.

Schott J. J. , Benson D. W., Basson C. T., Pease W., Silberbach G. M., Moak J. P., Maron B. J., Seidman C. E., Seidman J. G. (1998). Congenital heart disease caused by mutations in the transcription factor NKX2-5. Science 281, 108–111.

Smith S. M. , Dickman E. D., Thompson R. P., Sinning A. R., Wunsch A. M., Markwald R. R. (1997). Retinoic acid directs cardiac laterality and the expression of early markers of precardiac asymmetry. Dev. Biol . 182, 162–171.

Stapleton H. M. , Klosterhaus S., Eagle S., Fuh J., Meeker J. D., Blum A., Webster T. F. (2009). Detection of organophosphate flame retardants in furniture foam and U.S. house dust. Environ. Sci. Technol . 43, 7490–7495.

Suzuki K. , Takahashi K., Nishimaki-Mogami T., Kagechika H., Yamamoto M., Itabe H. (2009). Docosahexaenoic acid induces adipose differentiation-related protein through activation of retinoid x receptor in human choriocarcinoma BeWo cells. Biol. Pharm. Bull . 32, 1177–1182.

Swift M. R. , Pham V. N., Castranova D., Bel l. K., Poole R. J., Weinstein B. M. (2014). SoxF factors and Notch regulate nr2f2 gene expression during venous differentiation in zebrafish. Dev. Biol . 390, 116–125.

Tran P. , Zhang X. K., Salbert G., Hermann T., Lehmann J. M., Pfahl M. (1992). COUP orphan receptors are negative regulators of retinoic acid response pathways. Mol. Cell. Biol . 12, 4666–4676.

van der Veen I. , de Boer J. (2012). Phosphorus flame retardants: Properties, production, environmental occurrence, toxicity and analysis. Chemosphere 88, 1119–1153.

Vogel B. , Meder B., Just S., Laufer C., Berger I., Weber S., Katus H. A., Rottbauer W. (2009). In-vivo characterization of human dilated cardiomyopathy genes in zebrafish. Biochem. Biophys. Res. Commun . 390, 516–522.

Wang X. , Osinska H., Gerdes A. M., Robbins J. (2002). Desmin filaments and cardiac disease: Establishing causality. J. Cardiac Failure 8, S287–S292.

Waxman J. S. , Yelon D. (2007). Comparison of the expression patterns of newly identified zebrafish retinoic acid and retinoid X receptors. Dev. Dyn . 236, 587–595.

Wobus A. M. , Kaomei G., Shan J., Wellner M. C., Rohwedel J., Ji G., Fleischmann B., Katus H. A., Hescheler J., Franz W. M. (1997). Retinoic acid accelerates embryonic stem cell-derived cardiac differentiation and enhances development of ventricular cardiomyocytes. J. Mol. Cell Cardiol . 29, 1525–1539.

Wu B.-J. , Chiu C.-C., Chen C.-L., Wang W.-D., Wang J.-H., Wen Z.-H., Liu W., Chang H.-W., Wu C.-Y. (2014). Nuclear receptor subfamily 2 group F member 1a (nr2f1a) is required for vascular development in zebrafish. PloS One 9, e105939.

Yozzo K. L. , Isales G. M., Raftery T. R., Volz D. C. (2013). High-content screening assay for identification of chemicals impacting cardiovascular function in zebrafish embryos. Environ. Sci. Technol . 47, 11302–11310.

Zhang Y. , Huang L., Wang C., Gao D., Zuo Z. (2013). Phenanthrene exposure produces cardiac defects during embryo development of zebrafish (Danio rerio) through activation of MMP-9. Chemosphere 93, 1168–1175.

Zheng L. , Xu T., Li D., Zhou J. (2015). A representative retinoid X receptor antagonist UVI3003 induced teratogenesis in zebrafish embryos. J. Appl. Toxicol . 35, 280–286.